*geologica*acta

First evidence of paleoearthquakes along the Carboneras Fault Zone (SE Iberian Peninsula): Los Trances site

E. MASANA[1]   **X. MORENO**[1]   **E. GRÀCIA**[2]   **R. PALLÀS**[1]   **M. ORTUÑO**[1]   **R. LÓPEZ**[1]   **O. GÓMEZ-NOVELL**[1]   **P. RUANO**[3,4]
H. PEREA[2,5]   **P. STEPANCIKOVA**[6]   **G. KHAZARADZE**[1]

[1]Departament Dinàmica de la Terra i de l'Oceà, Grup RISKNAT, Universitat de Barcelona
Carrer Martí Franquès s/n, 08028 Barcelona, Spain.   Masana E-mail: eulalia.masana@ub.edu

[2]B-CSI, Institut de Ciències del Mar-CSIC
Pg. Marítim de la Barceloneta 37-49, 08003 Barcelona, Spain.   Gràcia E-mail: egracia@icm.csic.es

[3]Departamento de Geodinámica, Facultad de Ciencias, Universidad de Granada
Avenida de la Fuente Nueva s/n, 18071 Granada, Spain

[4]Instituto Andaluz de Ciencias de la Tierra (CSIC-UGR)
Avenida de la Fuente Nueva s/n, 18071 Granada, Spain.   Ruano E-mail: pruano@ugr.es

[5]GRD, Scripps Institution of Oceanography - University of California San Diego
8622 Kennel Way, La Jolla, CA 92093, United States.   Perea E-mail: hperea@ucsd.edu

[6]Institute of Rock Structure and Mechanics, Czech Academy of Sciences
V Holesovickach 41, 18209 Prague, Czech Republic.   Stepancikova E-mail: stepancikova@irsm.cas.cs

┤ **A B S T R A C T** ├

Seismogenic faults that have not produced historical large earthquakes remain unnoticed and, thus, are dangerously left out from seismic hazard analyses. The seismogenic nature of the Carboneras Fault Zone, a left-lateral strike-slip fault in the Eastern Betic Shear Zone (southeastern Spain), has not been fully explored to date in spite of having a morphological expression equivalent to the Alhama de Murcia Fault, a seismogenic fault in the same tectonic system. This study provides the first paleoseismic evidence of the seismogenic nature of the Carboneras Fault Zone, based on the analysis of 3 trenches at Los Trances site, on the northwestern edge of the La Serrata Range. Cross cutting relationships and numerical dating, based on radiocarbon, thermoluminescence and U-series, reveal a minimum of 4 paleoearthquakes: Paleoearthquake1 (the oldest) and Paleoearthquake2 took place after 133ka, Paleoearthquake3 occurred between 83–73ka and Paleoearthquake4 happened after 42.5ka (probably after 30.8ka), resulting in a maximum possible average recurrence of 33ka. This value, based on a minimum amount of paleoearthquakes, is probably overestimated, as it does not scale well with published slip-rates derived from offset channels or GPS geodetical data. The characterization of this fault as seismogenic, implies that it should be considered in the seismic hazard analyses of the SE Iberian Peninsula.

INTRODUCTION

Preparedness in the face of future earthquakes in a given region entails the detection and characterization of its potential seismic sources. Many seismogenic faults can be detected by analyzing the seismic catalogues (instrumental or historical). However, seismogenic faults found in areas affected by slow rates of stress accumulation (implying low slip-rates) are much more elusive, because they have remained silent during the historical and instrumental periods. Paleoseismology, in these cases, can be used to determine the seismogenic nature of such faults by detecting the effects of large prehistoric earthquakes in the geological record. Following this approach, a small number of faults in highly vulnerable areas of Western Europe, including the Iberian Peninsula, have been characterized

as seismogenic. Still many more faults of this kind need to be investigated to help quantify their associated hazard.

The Carboneras Fault Zone (CFZ), in southeastern Spain, is located at the southern tip of the Eastern Betic Shear Zone (Figs. 1; 2). With a length of 50km onshore and 90km offshore, it is one of the longest structures of this shear zone (Comas *et al.*, 1995; Gràcia *et al.*, 2006). The CFZ has not been considered to involve a seismic hazard in the region owing to its very low associated instrumental seismicity. However, it: i) reveals similar geomorphological features to those observed at the neighboring Alhama de Murcia Fault, which is proven to be seismogenic (Martínez-Díaz *et al.*, 2003; Masana *et al.*, 2004; Ortuño *et al.*, 2012; Ferrater *et al.*, 2017); ii) deforms young Quaternary deposits onshore and offshore
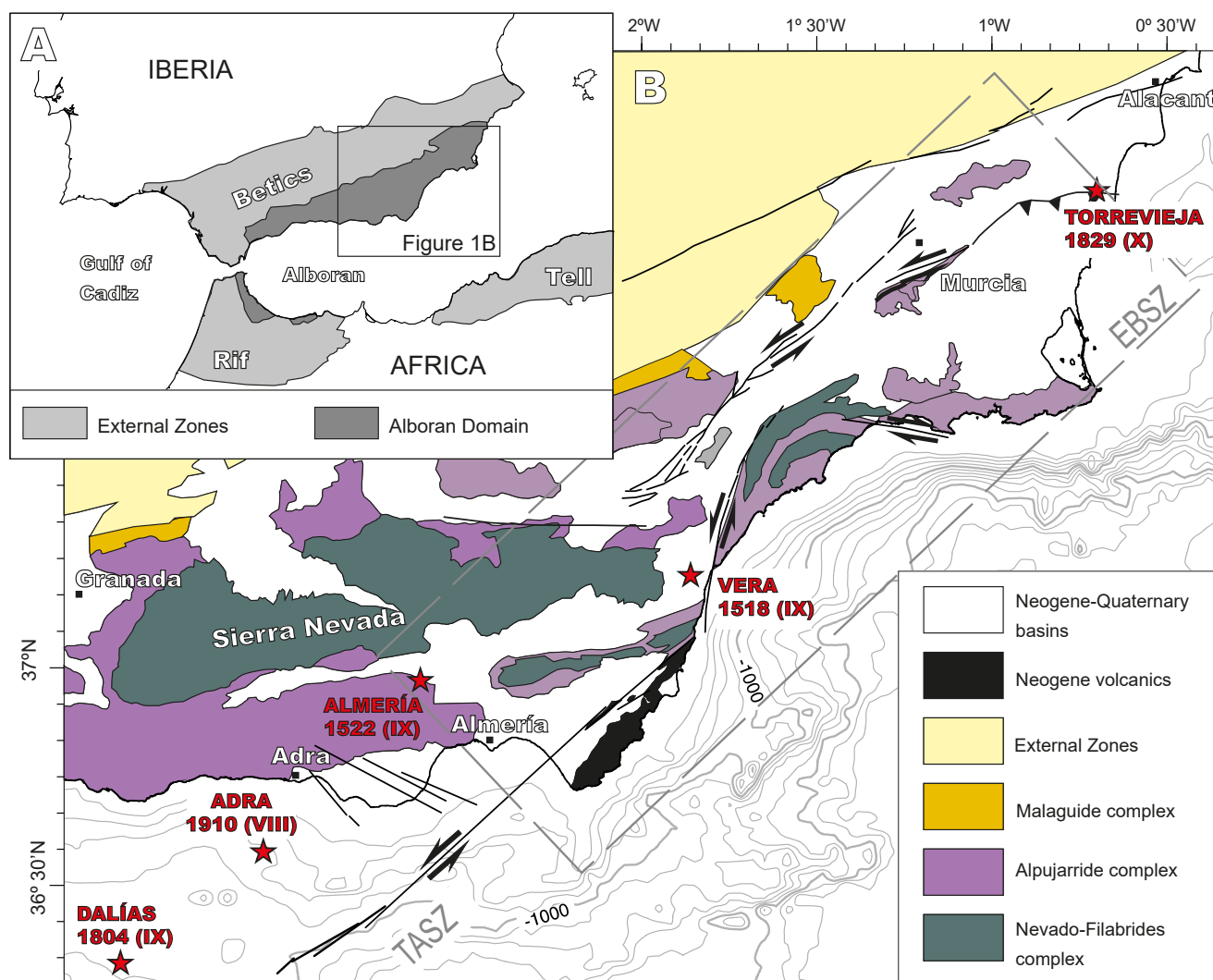
FIGURE 1. A) Map of the westernmost Mediterranean with the main Neogene onshore contractional ranges; B) Simplified geological map of the eastern Betics with the main structural units and the location of the Eastern Betic Shear Zone (EBSZ, within a dashed rectangle) and Trans-Alboran Shear Zone (TASZ). Red stars indicate the epicentral location of the historical largest earthquakes with its year and intensity value (Mezcua *et al.*, 2013). Thin grey isolines in the offshore area indicate the bathymetry in meters.

(possibly Holocene in age) (Gràcia *et al.*, 2006; Reicherter and Hübscher, 2007; Moreno, 2011; Moreno *et al.*, 2015, 2016) and iii) yields surprisingly high slip rates for the late Quaternary, 1.3mm/yr for the last 110ka (Moreno *et al.*, 2015).

The present paper builds upon the geomorphological, geochronological and neotectonic study of the CFZ at the La Serrata Range by Moreno *et al.* (2015). These authors indicated that the NW boundary of this range displays extensive and locally deformed Quaternary deposits overlying the fault trace, with moderate sedimentation-erosion ratios that makes it suitable for a paleoseismological study. Our study focuses on the CFZ at this boundary of La Serrata section, at Los Trances site, with the aim of demonstrating its seismogenic behavior and obtaining its first earthquake history. The resulting paleoseismological dataset is essential for a more realistic seismic hazard modeling and risk assessment in the region.

BACKGROUND

Regional setting

The Betics in southern Spain, together with the Rif in northern Africa, represent an arcuate shaped fold-and-thrust belt (Fig. 1) where Africa and Eurasia tectonic plates converge with a relative velocity ranging from 4.8 to 5.4mm/yr (Reilinger and McClusky, 2011; Argus *et al.*, 2011). The region is characterized by a
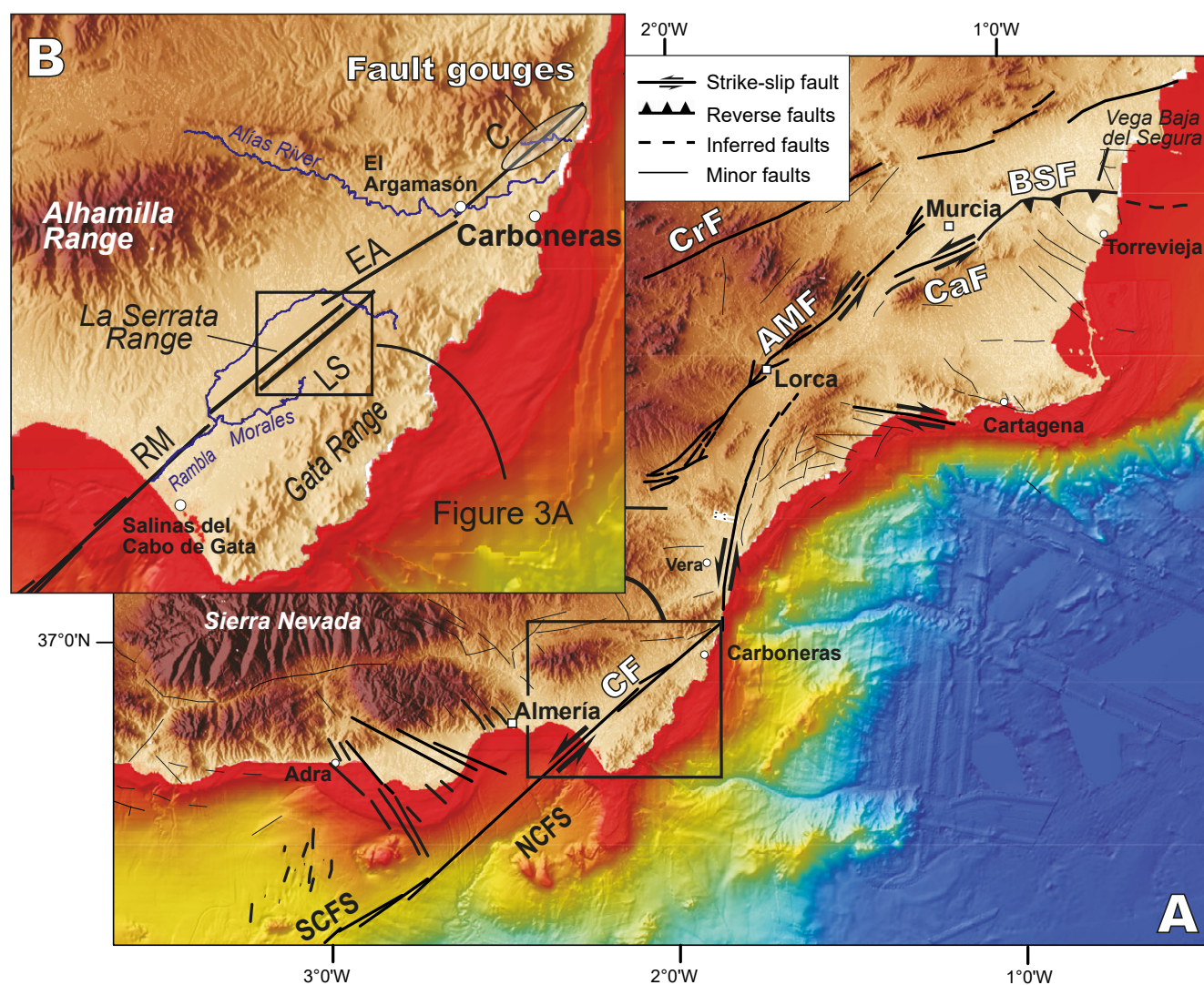
FIGURE 2. A) Topographic and bathymetric map of the Eastern Betic Shear Zone with indication of the main active faults. From North to South: AMF: Alhama de Murcia Fault; BSF: Bajo Segura Fault; CaF: Carrascoy Fault; CFZ: Carboneras Fault Zone; CrF: Crevillente Fault; PF: Palomares Fault. The CFZ offshore includes the South Carboneras Fault (SCFS) and North Carboneras Fault (NCFS) sections (Moreno *et al.*, 2016); B) Closer view of the northeastern part of the Carboneras Fault Zone with the four sections proposed by García-Mayordomo (2005): C: Carboneras; EA: El Argamasón; LS: La Serrata; RM: Rambla Morales. The black outlined square shows the location of Figure 3A.

diffuse shallow to deep seismicity of small to moderate magnitude earthquakes (Stich *et al.*, 2003a; Martín *et al.*, 2015), spanning approximately a 400km wide zone from the Rif to the Betics. In eastern Iberia, most of present-day shortening is accommodated by the Eastern Betics Shear Zone (Bousquet *et al.*, 1975; Bousquet, 1979; De Larouzière *et al.*, 1988; Sanz de Galdeano, 1990). This shear zone deforms the Internal Zones of the Betics, also referred to as the Alboran Domain (*e.g.* Booth-Rea *et al.*, 2007). It is composed by major NE- to ENE-trending, left-lateral strike-slip faults and E-W reverse faults at its northeastern end, from North to South: Bajo Segura, Alhama de Murcia, Palomares and CFZ (Figs. 1; 2). The CFZ enters about 90km into the Alboran Sea and is part of what has been defined as the Trans-Alboran Shear Zone, first described by Frizon de Lamotte *et al.* (1980) and De Larouzière *et al.* (1988). This last shear zone connects north-African extensional and transtensional faults such as Bokkoya and Trougout faults (Lafosse *et al.*, 2017), the Al-Idrissi fault system and strike-slip faults of the Djibouti plateau (Martínez-García *et al.*, 2013), with the Adra (Gràcia *et al.*, 2012) and CFZs in Almeria at the Iberian margin (Gràcia *et al.*, 2006; Moreno *et al.*, 2016).

The seismicity in the Iberian Peninsula is moderate and mostly concentrated on the Betics where large historical and instrumental earthquakes have occurred, such as the 1518 I_{EMS98} VIII-IX Vera earthquake, the 1522 I_{EMS98} VIII-IX Almería earthquake, the 1804 I_{EMS98} VIII-IX Dalías earthquake, the 1829 I_{EMS98} IX-X Torrevieja earthquake, the 1884 I_{EMS98} IX-X Arenas del Rey earthquake, the 1910 Adra earthquake (Mw 6.1) (Stich *et al.*, 2003b; Perea *et al.*, 2012; Mezcua *et al.*, 2013) and the recent 2011 Lorca earthquake (Mw 5.2) (Vissers and Maijninger, 2011; López-Comino *et al.*, 2012). In the Moroccan margin, the most relevant seismic events are the 1994 (Mw 6.0) (Calvert *et al.*, 1997) and 2004 (Mw 6.3) (Tahayt *et al.*, 2009) Al-Hoceima earthquakes, and the 2016 Al-Idrissi earthquake (Mw 6.4) (Buforn *et al.*, 2017) in the offshore.

The Carboneras Fault Zone (CFZ)

The CFZ (Bousquet *et al.*, 1975; Bousquet and Philip, 1976) is a N50-65° striking left-lateral fault (Fig. 2) that extends to the lower crust, with a maximum brittle break depth around 15km (Pedrera *et al.*, 2010). It is composed (Keller *et al.*, 1995) by an array of first-order subvertical NE-trending left-lateral strike-slip faults and by another array of second-order E- to ENE-trending faults that show an added reverse component. The width of the fault zone varies from a few hundred metres to about 2km at La Serrata Range. It is formed by overstepping and *en echelon* faults showing structures (pressure ridges, shutter-ridges, deflected drainages, sag ponds, water gaps and *en echelon*

folds), both onshore (Moreno *et al.*, 2015) and offshore (Gràcia *et al.*, 2006; Moreno *et al.*, 2016) that denote a recent transpressive deformation also evidenced by micro and macrostructures along the fault zone (Bousquet *et al.*, 1975; Fournier, 1980; Rutter *et al.*, 1986: Keller *et al.*, 1995). The motion of the CFZ began at the early Miocene (Fournier, 1980; Hall, 1983; Weijermars, 1987; Sanz de Galdeano, 1990; Vegas, 1992; Scotney *et al.*, 2000) and has persisted to the Quaternary (Bousquet *et al.*, 1975; Bousquet and Philip, 1976) and possibly to the Holocene, as suggested by Moreno *et al.* (2015).

Hall (1983) proposed 35–40km of strike-slip (and 5–6km of vertical slip) for the CFZ since the Burdigalian (15.9–20.4Ma), which implies a slip-rate of 1.7–2.5mm/yr. This is in agreement with studies based on the apparent offset of volcanic rock outcrops (Rutter *et al.*, 1986; Montenat and Ott D'Estevou, 1996) and with the 2mm/yr minimum slip-rate inferred by Montenat *et al.* (1990) based on the 18km displacement defined on an upper Tortonian/lower Messinian olistrostrome ("brèche rouge") along the CFZ.

Integration of onshore and offshore data suggests two major fault sections owing to its trace orientation: a northeastern N047 trending section and a southwestern N059-050 trending section entirely placed offshore (2B). In the onshore of the first fault section, García-Mayordomo (2005), in a study devoted to seismic hazard analysis, proposes 4 minor-scale sections in accordance with the fault trace continuity its surface geomorphological expression and the presence of minor N-S and NW-SE faults. These fault sections are, from North to South, Carboneras, El Argamasón, La Serrata (site of this study) and Rambla Morales, each of them about 10–14km of length (Fig. 2B). However, it is unclear if those sections are real seismogenic segments or they are well connected in depth in such a way that they easily can produce ruptures that can cross their edges during earthquakes. Even though the CFZ is a left-lateral fault, at La Serrata section, where Los Trances is located, shows a reverse component of motion that has derived in the uplift of the La Serrata Range.

Historically, a number of damaging earthquakes (*e.g.* 1487, 1518, 1522, 1804 and 1910) have destroyed the nearest cities and towns (*e.g.* Almería, Vera and Berja)(*e.g.* Udías *et al.*, 1976; Bousquet, 1979). Estimated intensities for these earthquakes range from VIII to X (Martínez-Solares and Mezcua, 2002; Mezcua *et al.*, 2013), and specifically are VIII (Almería 1487, Adra 1910) and VIII-IX, (Vera 1518, Almería 1522, Dalías 1804). The CFZ has been proposed as apossible source of the 1522 earthquake based on possible sea bottom surface ruptures (Reicherter and Hübscher, 2007), but the epicentral location is uncertain. During the instrumental period, scarce low to moderate magnitude earthquakes have been recorded

along the fault trace. Recent damaging events (Mw from 4.1 to 6.1) have been associated to minor NW-SE and N-S faults located northwest of the CFZ (Adra 1910, Adra 1993-1994; Rodríguez-Escudero *et al.*, 2014).

In spite of this scarce seismicity, the CFZ shows evidence of its Quaternary cumulative activity. Onshore, Quaternary deposits along the fault show horizontal and oblique slikensides revealing a horizontal motion with some vertical component (Bousquet, 1979). Faulted and vertically separated Tyrrhenian (early late Pleistocene; Goy and Zazo, 1983) marine terraces suggest a vertical slip-rate between 0.05 and 0.1mm/yr at the southwestern tip of the onshore fault (Rambla Morales area) and 0.05mm/yr at its northeastern tip (Carboneras area) (Bell *et al.*, 1997). Offshore, sea bottom scarps have been described that suggest recent fault-related ruptures (Estrada *et al.*, 1997; Gràcia *et al.*, 2006; Reicherter and Hübscher, 2007; Moreno *et al.*, 2016).

Moreno *et al.* (2016), assuming the entire rupture (140km) of the CFZ, calculate a maximum possible earthquake of Mw 7.6 ±0.3 (based on Wells and Coppersmith, 1994, scaling laws).

La Serrata section

The CFZ is mainly a left-lateral strike-slip structure (Bousquet, 1979). However, at La Serrata section, it also shows evidence of a vertical component, such as a positive flower structure or restraining step-overs that crop out extensivelly along the La Serrata Range.

La Serrata Range is a 14km long and 1km wide elongated range bounded by two main parallel faults of CFZ (Weijermars, 1991; Bell *et al.*, 1997; Silva *et al.*, 2003). These faults show a main left-lateral strike-slip sense of motion added to a minor reverse component (Fig. 2). The range is made up of Pliocene conglomerates (Bell *et al.*, 1997) and Neogene volcanic and marine-sedimentary deposits that unconformably overlie Paleozoic and Mesozoic rocks of the Internal Betics. In particular, phyllites, quartzites and dolomites of the Alpujarride Complex and limestones, lutites and sandstones of the Malaguide Complex (Pineda *et al.*, 1981; Boorsma, 1992; Fernández-Soler, 1996; Vera, 2000).

The fault bounding La Serrata Range to the NW shows a discontinuous pressure ridge where Pliocene rocks crop out (Fig. 3A) (Bell *et al.*, 1997) and a fault zone up-to 200m wide with constant step-overs.

A systematic left-lateral deflection of drainages is remarkable, especially along the NW La Serrata range boundary (Baena *et al.*, 1977; Bousquet, 1979; Goy and

Zazo, 1983; Weijermars, 1991; Boorsma, 1992; Bell *et al.*, 1997). Bell *et al.* (1997) suggest that left-lateral displacements in the order of 80-100m took place there at least since 100ka, most probably during the middle Pleistocene (125–700ka). Assuming a mean age of 500ka, the average lateral slip-rate calculated by these authors is 0.2–0.3mm/yr. They did not report evidence of movements younger than 35–100ka. In contrast, Moreno *et al.* (2015), interpreting a number of left laterally deflected channels along La Serrata Range, proposed a minimum left-lateral slip-rate of 1.31mm/yr since 110.3ka, which is in agreement with the rate obtained by GPS measurements (Echeverria *et al.*, 2015). In addition, Moreno *et al.* (2015) suggested dislocation of a dated Holocene fluvial channel at El Hacho site (Fig. 3A), indicating that a fault movement may have taken place later than 637yr AD.

Continental alluvial fans and fluvial sediments, fed by the La Serrata Range, characterize the Quaternary record at both sides of La Serrata Range. Alluvial fans were initially grouped into different generations attributed to the Pleistocene and Holocene (Pineda *et al.*, 1981; Goy and Zazo, 1983, 1986; Schulte, 2002; Maher *et al.*, 2007; Santisteban and Schulte, 2007). Rodés *et al.* (2011) dated the lower generation using cosmonuclide (^{10}Be), obtaining an age between 200ka and *ca.* 1Ma (1σ 1Ma (*ca.* 200 an age). More recently, Moreno *et al.* (2015) constructed a chronological framework for these alluvial and fluvial units based on 42 new numerical ages combined with the regional climatic model of alluvial deposition in SE Iberia. In this framework, they distinguished 4 main phases of alluvial fan aggradation (A1 to A4) and 2 phases of fluvial deposition (F1, F2) in La Serrata Range area (Fig. 3). These are, from bottom to top:

i) The A1 alluvial fans, interpreted as likely early to middle Pleistocene in age, with a minimum age between *ca.* 1–0.35Ma.

ii) The A2 alluvial fans, interpreted as being deposited during the cold stages of the middle Pleistocene, with a last aggradation pulse that probably occurred during Marine Isotopic Stage (MIS) 6 (191–130ka). In concordance with the numerical dates, unit A2 is 133–56.7ka old.

iii) The F1 fluvial deposits, which were formed during the late Pleistocene within the MIS 5 and during MIS 4 (130–57ka) and yield ages constrained between 83 and 45.5ka.

iv) The A3 alluvial fans show two sequences from bottom to top, A3.1 and A3.2, being the former the only one in contact with the fault (and the only dated). These alluvial fans were formed during the late Pleistocene glacials of MIS 4 and MIS 2 (71–14ka) with A3.1 yielding
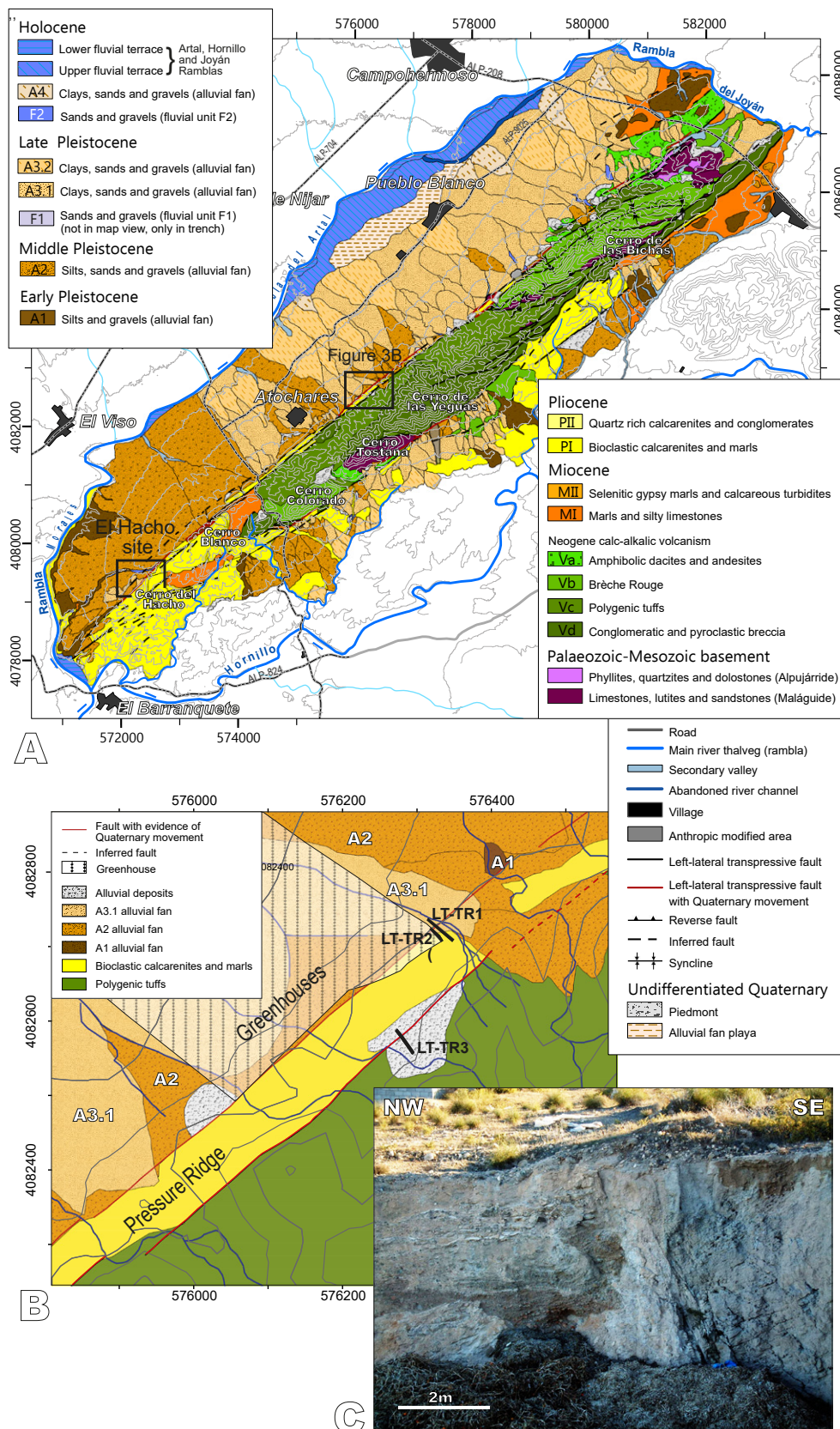
FIGURE 3. A) Geological map of La Serrata Range area (modified from Moreno *et al.*, 2015) with the location of the Los Trances site (Fig. 3B). See map location in Figure 2B; B) Detail of the geological map at the Los Trances site with the position of studies trenches 1, 2 and 3 (LT-TR-1, LT-TR-2 and LT-TR-3); C) Photography of the fault damage zone of Trench 2 (see Fig. 4A for details on the observed structure and stratigraphy).
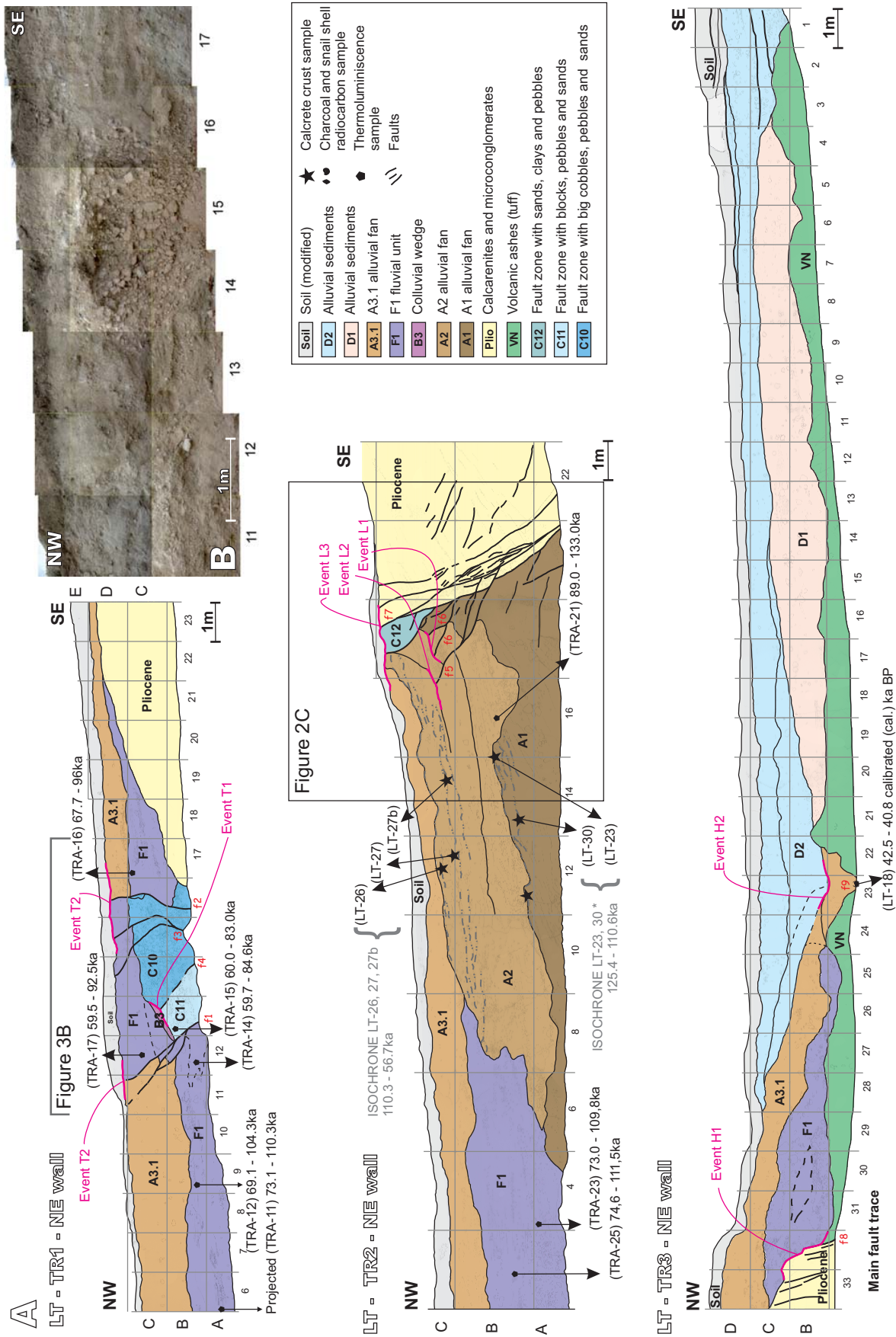
FIGURE 4. A) Geologic logs of the northeast walls of trenches 1 (LT-TR1-NE), 2 (LT-TR2-NE) and 3(LT-TR1-NE) with the position of the dated samples and obtained ages (analyses details on Tables 1, 2, 3). Thick pink lines in the sections indicate the horizons post-dating the identified earthquake events (pink texts). Coordinates of each square drawn in the log are indicated by capital letters for the horizontal raws (A, B, C and D) and numbers for the columns in each trench photomosaic. See location of the 3 trenches in Figure 3B; B) Detail of the photomosaic of the fault damage zone in trench 1.

an age of aggradation between 71.6 and 20.6ka and likely younger than 30.8ka.

v) And, finally, fluvial channels (F2), entrenched on top of A3 fans, where dated as 1313-929yr BP (paleochannel infill at El Hacho site) and as 1413-744yr BP (Fig. 3A).

METHODS

Obtaining relevant paleoseismological data largely relies on accurate selection and analysis of trenching sites. Geological and Geomorphological mapping at 1:10,000 scale (described in Moreno *et al.*, 2015) allowed the selection of Los Trances site as a suitable area for a paleoseismological study (Fig. 3B), as the trace of the NW La Serrata Range bounding fault is in coincidence with the most recent alluvial units.

Three parallel trenches were dug and analyzed at this place. Trenches were 20–30m long and 2.5–3m deep, but a pre-existing 5m high anthropic wall was also cleaned and used for paleoseismological analysis (trench 2). After cleaning of the walls, reference grids for logging were installed using nylon string at 1m spacing at trenches 1 and 3 and at 2m at trench 2. Series of photographs of every grid cells were obtained and then retro-deformed using Photoshop software and assembled to construct photo-mosaics (Fig. 4). The resulting 2D image model of each trench wall was used in the field as a reference graphic record to log at a 1:20 scale the stratigraphic, pedogenic and tectonic limits. Finally, the interpreted log was digitized to obtain an image that synthesizes the paleoearthquake history resulting from the trench wall analysis (Fig. 4A).

Sedimentary units cropping out on trench walls were sampled for radiocarbon, thermoluminescence (TL), and U-series dating, depending on the availability of suitable material. A detailed account on the sampling criteria, on the materials used for dating and on the resulting numerical ages of Quaternary units of regional extent is reported in Moreno *et al.* (2015).

RESULTS

Los Trances site

Los Trances site is located in the central part of the NW Serrata Range boundary (Fig. 3A), which is constituted here by Neogene volcanic rocks (polygenic tuffs and conglomeratic breccias). The fault bounding La Serrata Range to the northwest splits here into two main parallel faults delimiting a pressure ridge made up of Pliocene quartz rich bioclastic calcarenites and marls (Fig. 4B). To

the northwest of this ridge, the thick calcrete crust on top of the A1 alluvial unit crops out locally at the bottom of a gully. A2 alluvial fans are in linear contact with the pressure ridge except in the NE of the area where several apexes overlie the fault zone. A3.1 alluvial fans were mostly deposited downhill from the pressure ridge, although their apexes are located locally beyond the trace of the northwestern fault.

In this setting, trenches 1 and 2 were placed across the trace of the fault bounding the pressure ridge to the NW, and trench 3 across the trace that limits this ridge to the southeast (Figs. 3B; 4). Trench 2 (a 5m high wall) facilitated the investigation of old events as it exposed a deep cross section of the NW fault, showing A1, A2 and A3 alluvial fans being thrusted by Pliocene rocks (Fig. 3C). Trench 1 was dug in younger deposits (F1 fluvial unit), to investigate faulting on the uppermost deposits (Figs. 3; 4). To obtain evidence of recent faulting along the fault bounding the pressure ridge to the southeast, trench 3 was opened where a young alluvial deposit covers the trace (TR3; Figs. 3; 4).

Los Trances Trench 1 (TR1)

The NE wall of this trench (Fig. 4) shows a 5m wide fault zone (both walls looked very similar). To the SE the quartz-rich Pliocene calcarenites contain interbedded microconglomerates of well-rounded quartz pebbles and abundant marine fossil shells. The F1 fluvial unit onlaps the Pliocene rocks and is faulted and uplifted in the fault zone showing a positive flower structure. Unit F1 is made up of light brown sandy matrix-supported conglomerates with millimetric to decimetric pebbles showing a good but irregular internal stratification, which suggests a fluvial process of formation (Moreno *et al.*, 2015). Pebbles are mainly of volcanic nature and define layers of alternating different sizes and cementation degree. Locally, some channel-shaped bodies of matrix-supported sand and orangey clay levels are observed within unit F1. Unit A3.1 (upper Pleistocene alluvial fan) overlies unit F1 and extends to the SE directly covering the Pliocene sediments. However, unit A3.1 is absent in the area between the main faults, probably because it was uplifted and eroded. On top of the trench wall and unaffected by the fault zone, a dark brown unit with pebbles, roots and high organic content was labeled as the current soil and may be partly reworked by human activity, so it will not be taken into account in the description of the events. The main faults (f1 and f2) bound units C10, C11 and B3 (Fig. 4). Unit C10 has a chaotic aspect made up of rounded cobbles (up to 25cm) with smaller pebbles and sand filling the interstitial spaces. Unit C11 is also composed of rounded cobbles but with a good internal stratification, interpreted as a slightly deformed fluvial unit. Both units probably correspond to lower layers of the deformed F1 fluvial unit and are clearly younger than A2 (in TR2) according to their composition

and to the absence of calcified layers, very abundant in A2 (see TR2 for a description of A2). Overlying the fault contact (f4) between C10 and C11, there is a loose, local and chaotic deposit, labeled B3, which is made up of angular Neogene volcanic pebbles of different sizes. According to its wedge shape and its coarse (and local) composition, this deposit was interpreted as the remains of a colluvial wedge associated with the fault zone. Other faults were revealed by this exposure (f3). The central part of this trench (columns number 12 to number 16 in the log; Fig. 4) is uplifted by two main faults (f1 and f2) with reverse separation that affect the complete sequence (owing to the long-term behavior of the CFZ).

The analysis of trench 1 shows young units involved in the fault zone and allowed us to differentiate two paleoseismic events (T1 and T2), postdating the A2 alluvial fan cropping out at trench 2 (Figs. 3; 4). Event T1 is evidenced by the upward termination of fault f4 sealed by unit B3 that might be the remnant of a colluvial wedge. Event T2 is evidenced by faults f1, f2 and f3 that affect units F1 and A3.1 and reach the surface.

Los Trances Trench 2 (TR2)

This trench shows a superimposition of A1, A2, F1 and A3.1 units (Fig. 4). Unit A1 is composed by a matrix supported conglomerate with a brown to ochre sandy matrix and dispersed quartz and volcanic pebbles, the later up to 30cm in size. Quartz pebbles are sub-rounded and the volcanic ones are sub-angular containing abundant hornblende crystals. Towards the top, this unit shows up to 50cm thick calcrete crust with different phases of laminated layers. The base of the conglomerates corresponding to the unit A2 is erosive on top of A1. A2 has paleochannels that are filled with decimetric well-rounded boulders of volcanic origin at the base grading upwards to centimetric-size pebbles. The upper parts of the channels are made up of a hardened clay-sandy pink matrix and contain well-rounded quartz pebbles changing into volcanic gravels upwards. A densely fractured calcrete crust is present on top of the unit with variable thickness, from centimetric to half a meter. The top of A2 is warped upwards next to the fault. In the NW part of the trench, unit F1 (fluvial deposits) overlies erosively units A1 and A2. Above, the A3.1 alluvial fan covers F1 and A2 deposits and does not reach the fault itself in this trench. Sands and clays with dispersed quartz and volcanic pebbles compose unit C12, located next to the main fault. It probably corresponds to a deformed A2 (or A1) strip.

The southeastern part of the trench shows a sharp fault (f7) bounding Pliocene and Quaternary deposits. The fault dips strongly to the southeast, has a reverse separation, and reaches the surface (soil was not considered as it shows

evidence of very recent reworking), cutting through units A1 and A2 and slightly folding up the complete sequence. Units F1 and A3.1 are not in contact with the fault but the southeastern edge of A3.1, next to the fault, is warped upwards. A number of reverse minor faults branch out from f7 affecting the top of A1 and the lower half of A2 (f5 and f6, respectively).

The analysis of trench 2 provided evidence for at least three paleoearthquakes (L1 to L3) (Figs. 3; 4). Event L1 is evidenced by the upward truncation of the two branches of f6, being sealed by the middle part of unit A2 close to the main fault zone. Event L2 is evidenced by the upward truncation of f5 being sealed by the calcrete crust of the upper part of unit A2 (the bottom of A3.1 is not either affected by f5). Event L3 is evidenced by offset and deformation along f7 that affects the calcrete layer developed on top of unit A2 and warps unit A3.1 (and affects unit C12).

Los Trances Trench 3 (TR3)

While the other two trenches where dug along the same fault trace, trench 3 (Fig. 4) was excavated across the trace that bounds to the southeast the pressure ridge (Fig. 3B), composed by Pliocene calcarenites and microconglomerates. Unit VN (Neogene volcanic ashes with light green to white tuffs and some interbedded light orange layers containing millimetric hornblende crystals) crops out at the bottom of the exposure except in its northwestern edge where the Pliocene deposits are separated from VN by a fault (f8). This fault is sealed by an underformed F1 deposit, which in turn is overlain by the A3.1 alluvial fan (northwestern edge of the trench log). Unit D1 and D2 composed by alluvial deposits, onlap on the previous sequence. At the bottom, D1 is made up of sands, clays and pebbles of different shapes and sizes. At the base of D1, millimetric and well-rounded pebbles form channels. In the middle of the unit, up to 10cm long angular pebbles are dispersed in slightly cemented clay to sandy matrix, with interbedded well-rounded pebbles. Towards the top, unit D1 becomes well consolidated. Overlying D1 and A3.1, there is unit D2 that shows a double channel-shaped morphology composed by loose dark brown to grey sandy matrix with plenty of millimetric to centimetric pebbles mainly of volcanic origin. The entire alluvial succession is covered by an undeformed pedogenic soil constituted by a dark brown sandy matrix with pebbles and fine roots.

Trench 3 shows two areas with evidence of deformation. The most evident is on its northwestern edge (f8), where Pliocene units are in sharp, almost vertical, contact with units VN and the lower part of F1. We interpreted this as a fault contact (f8; Fig. 4). The upper part of F1 onlaps the

TABLE 1. Radiocarbon dating results

				Radiocarbon dating from a Snail shell						
Sample name	Sample type	Unit	Laboratory	Lab. Ref.	Detection method	$^{13}C/^{12}C$ (‰)	Conventional ^{14}C age 2σ (ka BP)	Calibrated age 2σ (calka BP)	Conventional ^{14}C age range 2σ (ka BP)	
LT-18	Snail shell	A3.1	Beta Analytic	244754	AMS	-7.6	37.2 ± 0.5	42.5 – 40.8	36.7 - 37.7	

eroded fault scarp developed on the Pliocene deposits and, thus, postdates the last movements of this fault. The other possible deformation zone is at column number 23 (f9; Fig. 4), where a N050E trending open crack filled with A3.1 sediments was identified in the irregular volcanic unit.

The paleoseismological analysis of this trench shows evidence for at least two paleoearthquakes (H1 and H2). The buried scarp on the Pliocene unit (f8) evidences event H1. Unit F1 does not show evidence of faulting near the fault and therefore the event took place likely before the deposition of F1. The fact that the scarp shows a buried free face in the Pliocene unit, which is here very loose, suggests that F1 may shortly postdate the event. The second event, H2, is based on a fault crack (f9; Fig.4) that is filled up with sediments of unit A3.1, suggesting an opening of the crack after the deposition of A3.1. However, considering that VN is cemented, the opening of the crack is not well constrained in time as it could have remained opened for a period of time and thus, the opening could be previous to A3.1. Unit D2, instead shows no evidence of deformation and, thus, postdates the event. This is a weak evidence for a paleoearthquake event as other processes, like terrain adjustments, may account for it.

Dating at Los Trances area

In the trenches at Los Trances, Moreno *et al.* (2015) used U-series to date calcrete crusts on top of units A1 and A2, thermoluminescence to date fine grained sediments from units A2, F1 and A3.1, and radiocarbon to date a charcoal fragment from unit A3.1 (Fig. 4; Tables 1; 2; 3). The U-series ages on the calcrete crust were calculated using isochrones. The authors suggested that these calcretes are often polygenic, with phases of precipitation of carbonates that take place long after initial precipitation.

Hence, they tend to yield younger ages than those of the final aggradation of the fan. These calcrete crusts were sampled and dated because, even if they do not provide an exact age of the alluvial fans, they predate the age of the calcrete crust rupture.

The timing of the paleoearthquakes was constrained by using the results from the samples in the Los Trances trenches taking into account their stratigraphic position (Fig. 5). Additionally, in the absence of other ages, we also used the ages and chronology of the regional units defined by Moreno *et al.* (2015). According to them, unit A1 has an age of 0.35–1Ma, unit A2 of 136–56.7ka, and unit F1 of 83–45.5Ka.

DISCUSSION

Time constraining of the event horizons

The age of each event horizon was constrained using the regional and local dates available (Fig. 5; Tables 1; 2; 3) as follows:

i) Event T1, in trench 1, took place after the deposition of units C10 and C11, dated by sample TRA15 (60.0–83.0TL ka). It predates units B3 and F1. The lowest sample dated in F1 unit is TRA23 (Trench 2, 73.0–109.8TL ka). Therefore, the age of Event T1 is constrained between 83 and 73ka.

ii) Event T2, in trench 1, is evidenced by faults f1, f2 and f3 that cut across all the sedimentary units up to the base of the present reworked soil and, hence, postdating units F1 and A3.1. A radiocarbon age (sample LT-18) was obtained at the base of unit A3.1 (42.5–40.8cal ka BP) long

TABLE 2. U-series dating results

								U-series from laminar calcrete					
Sample name	Lab code	Unit	U-238 (ppm)	Th -232 (ppm)	$^{234}U/^{238}U$	$^{230}Th/^{232}Th$	$^{234}U/^{232}Th$	$^{238}U/^{232}Th$	$^{230}Th/^{234}U$	Nominal date (ka BP)	Nominal date range (ka BP)	Isochronage (ka BP)	Isochron age range (ka BP)
LT-27b	2508	A2	1	0.47	1.27	6.216	8.359	6.596	0.74	13.7 +6.8/-6.5	7.2 – 20.5	80.5 +29.8/-23.8	56.7 – 110.3
LT-27	3308	A2	0.67	0.39	1.31	6.01	7.059	5.393	0.85	18 +11.2/-10.3	7.7 – 29.2		
LT-26	2108	A2	0.53	0.37	1.22	4.642	5.357	4.408	0.87	19.4 +16/-14.1	5.3 – 35.4		
LT-23	2008	A1	1.55	0.57	1.36	9.437	11.558	8.491	0.82	162.3 +12.8/-11.6	150.7 – 175.1	117.7 +7.6/-7.2	110.5– 125.3
LT-30	2408	A1	1.29	0.22	1.42	18.910	25.539	17.992	0.74	132.7 +6.2/-5.9	126.8 – 138.9		

predating event T2. An additional sample (HAC-17) was dated on top of A3.1 unit at El Hacho site (Moreno *et al.*, 2015) suggesting that the top of unit A3.1 would have been deposited after 30.8TL ka. According to this, Event T2 would have occurred after 30.8ka.

iii) Event L1, in trench 2, is evidenced by the upper truncation of faults f6 and f6'. Sample TRA21 (89.0–133.0TL ka) underlies the event horizon and provides a good maximum age estimate for the event. The isochrone drawn from calcrete samples LT26, 27 and 27b (Moreno *et al.*, 2015) yield an age (110.3–56.7U-series ka), which postdates the event. Hence, event L1 took place between 133.0ka and 56.7ka. This is consistent with the older age regionally obtained for the aggradation phase of unit A1 (0.35–1Ma) by Moreno *et al.* (2015).

iv) Event L2 is younger than event L1 but cannot be discriminated. According to the available dates (see Event L1), it occurred also between 133.0 and 56.7ka.

v) Event L3 is younger than Event L2 and the calcrete crusts on top of unit A2. It is also younger than unit A3.1 according to the fact that this unit is warped next to the fault. Based on the age constraints on A3.1 (Moreno *et al.*, 2015) event L3 occurred later than 30.8ka.

vi) Event H1 took place little before the deposition of unit F1 and after unit VN. There is no age constraint for VN and the (stratigraphically) lowest sample at unit F1 is TRA23 (trench 2), which indicates that this event may have occurred little before 73ka.

vii) Event H2 is uncertain as an event and has a weak chronology (see discussion in description of the events). Despite this, if we consider the most likely interpretation, it occurred after the deposition of sample LT18 (42.5–40.8cal ka BP) in unit A3.1. Therefore, we suggest that event H2 occurred after 42.5ka.

Correlation of events

Observation along the three analyzed trenches provides evidence for 7 rupture events, each of which ischronologically constrained. No more than three consecutive events are observed from any single trench. The analysis of the complete dataset suggests that all events can result from a minimum of 4 paleoearthquakes (Fig. 5), which we label Pqk1 to Pqk4, from old to young. Pqk1 is deduced in trench 2 and corresponds to Event L1. It would be younger than 133ka and, based on its stratigraphical position, older than Pqk2. Event L2 evidences Pqk2 in trench 2 and is, based on its stratigraphical position, younger than Pqk1 and older than Pqk3. Pqk3 is based on the correlation of events T1 (in trench 1) and H1 (in

trench 3), as both ruptures would have taken place shortly before the deposition of units B3 and F1. It is constrained as taking place in the period 83–73ka. Finally, Pqk4 is deduced from Events T2 (observed in trench 1), L3 (in trench 2), and the doubtful H2 (in trench 3). No layer other than the reworked soil overlaps horizon events T2 and L3 (f2, f3, f1 and f7 appear to be truncated), whereas the younger unit D2 covers horizon event H2. However, all these events postdate at least the bottom of unit A3.1, and no evidence is found to attribute them to more than a single paleoearthquake. Based on the age of top of unit A3.1, Pqk4 took place later than 30.8ka. According to the correlation of events and their time constraints, a synchronous activity of the two analyzed fault traces is suggested.

The seismic potential of the Carboneras Fault Zone (CFZ)

Evidence of at least 4 paleoearthquakes was found in three trenches at Los Trances site. Events were interpreted based on fault terminations, a colluvial wedge, an open crack and a buried scarp. Further paleoseismic studies should confirm the lateral extent of these ruptures and the possible segmentation of the fault.

Previous studies (Reicherter and Hübscher, 2007; Moreno *et al.*, 2016) have already suggested that the CFZ ruptures the sea floor and that it is a potential source of the 1522 Almeria earthquake. Our study provides the first *in situ* paleoseismic evidence of the seismogenic nature of this fault zone by means of a paleoseismological analysis. The thick fault gouge described at the CFZ northestern end (Faulkner *et al.*, 2003; Rutter *et al.*, 2012; Fig. 2B) suggest an aseismic behavior, in contrast to the now proved seismogenic La Serrata section. Faulkner *et al.* (2003) suggested that the fault might behave differently as a function of the basement rocks involved in the fault gouge. These authors proposed a mixed mode seismic signature for the CFZ by comparing it to particular segments of the San Andreas Fault, which move both seismically and by creep. In the CFZ case, earthquakes would nucleate in the fault zone developed over the bedrock brittle portions, whereas the phyllosilicate-rich

TABLE 3. Thermoluminiscence dating results

Thermoluminescence (TL) dating from fine-grained sediments				
Sample name	Trench outcrop	Unit	TL age (ka BP)	TL age ranges (ka BP)
HAC-17	EH-TR2	A3.1	28.7 +2.1/-1.8	26.9 – 30.8
TRA-11	LT-TR1	F1	87.9 +22.4/-14.8	73.1 – 107.3
TRA-12	LT-TR1	F1	83.3 +21.0/-14.2	69.1 – 104.3
TRA-14	LT-TR1	F1	70.2 +14.4/-10.5	59.7 – 84.6
TRA-15	LT-TR1	F1	69.8 +13.2/-9.8	60 - 83
TRA-16	LT-TR1	F1	79.4 +16.6/-11.7	67.7 - 96
TRA-17	LT-TR1	F1	73.1 +19.4/-13.6	59.5 – 92.5
TRA-23	LT-TR2	F1	87.7 +22.1/-14.7	73 – 65.6
TRA-25	LT-TR2	F1	89.3 +22.2/-14.7	74.6 – 111.5
TRA-21	LT-TR2	A2	106 +27/-17	89 - 133
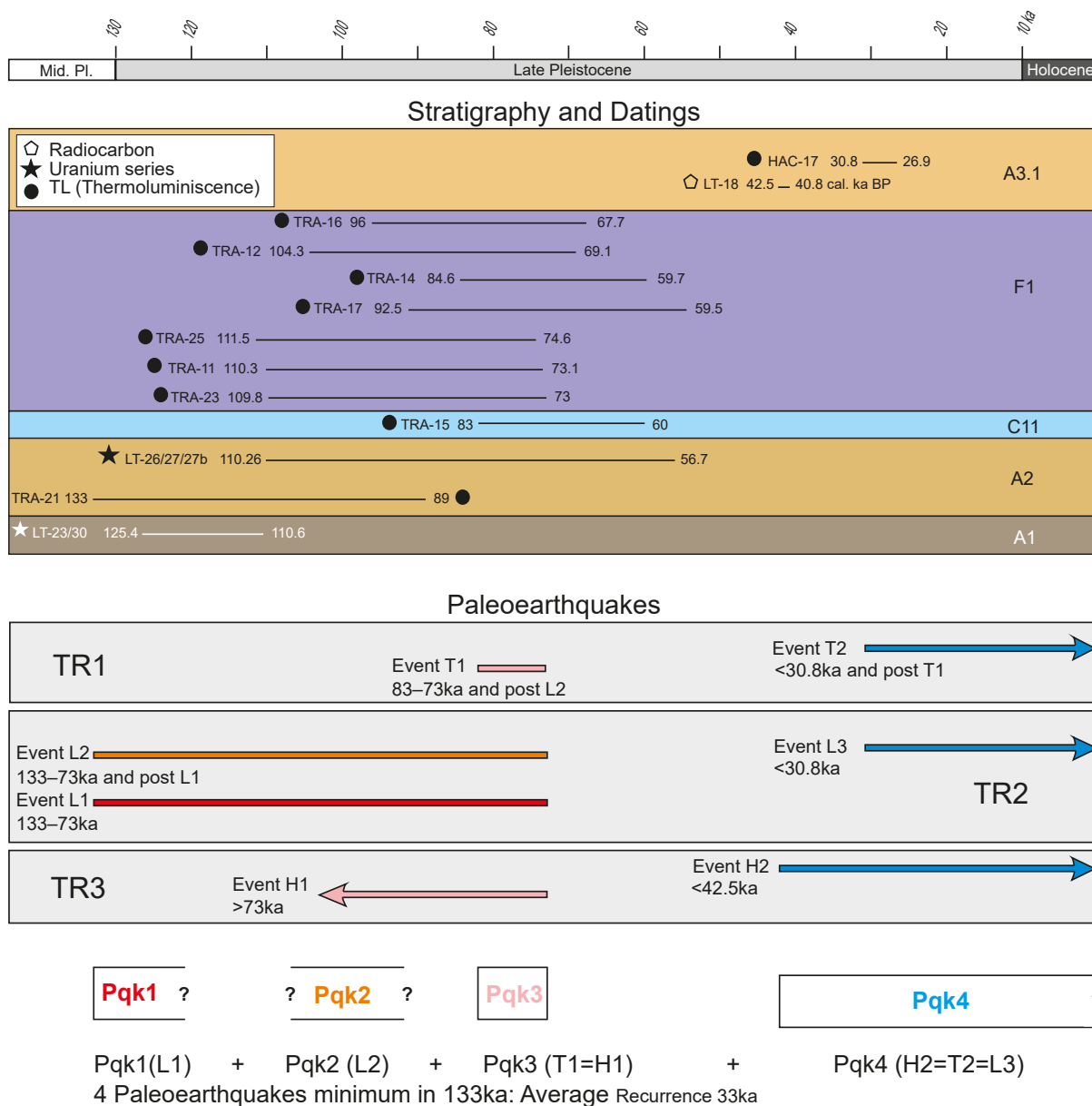
FIGURE 5. Chronological chart with, from top to bottom of the figure, i) the stratigraphy (A1, A2, C11, F1 and A3.1) and the age of the dated samples, ii) the paleoseismic events observed in each trench with their assigned age (T1 and T2 in TR1, L1 to L3 in TR2, and H1 and H2 in TR3); and iii) the minimum possible amount of paleoearthquakes (Pqk1 to Pqk4) that can be inferred from the correlation among these events. In brackets, the observed events assigned to each paleoearthquake.

fault gouge would behave as a creeping zone. More recently, Rodríguez-Escudero (2017) proposed a rupturing model for the Alhama de Murcia Fault (Figs. 1; 2) that might also apply to the CFZ. This model, inspired in laboratory tests performed by Niemeijer and Niemeijerand Vissers (2014) and Rodríguez-Escudero (2017), proposes that seismogenic ruptures nucleate in the resistant parts of the fault zone, but can propagate through the more ductile parts. This would happen when the energy of the earthquake and its propagation velocity are large enough to trigger frictional hardening effect on the fault gouge.

The sequence deduced of 4 paleoearthquakes starting at 133ka or later (the age of Pqk1), yields a maximum value of 33ka for the mean recurrence interval of earthquakes along the CFZ. However, this paleoearthquakes sequence is based on the simplicity principle. So, an occurrence of 7 earthquakes (a different one per each rupture event identified in the 3 trenches) cannot be ruled out. This scenario would imply a maximum value for the mean recurrence interval of 19ka. Even considering 7 events, the resulting recurrence does not scale with the slip-rate along the fault of 1.3mm/yr since 110ka, deduced from

geomorphological analysis by Moreno *et al.* (2015), as it would imply an unrealistic slip per event larger than 24m. This mismatch strongly suggests that the Los Trances site is not representative of the complete rupturing history of the fault zone.

Two main causes might be called to explain the suspected lack of completeness of the paleoseismic record. On one side, the discontinuous character of sedimentation in the sites studied can only provide part of the history of the fault: two rupturing events constrained by the same stratigraphic markers, for instance, cannot be disclosed. On the other side, magnetotelluric models across La Serrata Range (Pedrera *et al.*, 2010) shows that the fault traces located on each side of it converge at depth to a narrower deformation zone. During a seismogenic event in the studied fault section, the deformation at depth might be partitioned among the two fault branches limiting the La Serrata Range flower structure. The paleoseismic results discussed in this paper derive only from the fault zone bounding La Serrata Range to the northwest. Thus, the paleoseismic results are minimum values on the assumption that the recent deformation may be distributed over the entire deformation zone. To obtain a more realistic idea of the paleoseismic parameters at La Serrata Range, all the fault traces should be taken into account and should be analyzed from a paleoseismic point of view.

The sequence of earthquakes described (Pqk1 to Pqk4) is not sufficiently constrained in time and is not complete enough to extract the possible fault behavior in terms of clustering or periodic recurrence. However, a minimum of three paleoearthquakes (Pqk1 to Pqk3) occurred in the period comprised between 133ka and 67ka, and only one (Pqk4), took place thereafter.

The left-lateral component of the CFZ hampers the analysis of slip per event based on trenches dug across to the fault (a 3D approach would be required). The structure observed in the Los Trances trenches mimics what has been described at a larger scale along the CFZ: a positive flower structure, with reverse faults being shallowly rooted into a highly dipping main fault that might absorb the main strike slip component of slip. This has been especially described in detail by high resolution seismic reflection along the offshore part of the fault (Moreno *et al.*, 2016).

CONCLUSIONS

Our results demonstrate that the Carboneras Fault Zone (CFZ) is seismogenic. It has produced a minimum of 4 paleoearthquakes during the last 133ka, with a resulting maximum possible average recurrence of 33ka. These values are likely an underestimation of the complete history of seismic surface ruptures of the CFZ, but constitute the first paleoseismic results in it. Evidence of surface rupturing paleoearthquakes (Mw>5, morphogenetic events) is observed on the two fault traces analyzed along the NW side of La Serrata Range, which bound the pressure ridge at Los Trances site. The paleoseismic parameters obtained are not scaled with the large slip-rates deduced from geomorphological and geodetic studies. This is consistent with the incompleteness of the paleoseismic history being recorded at Los Trances site and suggests that active deformation is also likely to be distributed along the opposite (SE) side of La Serrata Range.

The characterization of the CFZ as seismogenic implies that it should be considered in seismic hazard analyses of the region.

REFERENCES

Argus, D.F., Gordon, R.G., DeMets, C., 2011. Geologically current motion of 56 plates relative to the no-net-rotation reference frame. Geochemistry, Geophysics, Geosystems, 12(11), Q11001. DOI: 10.1029/2011GC003751

Baena, J., Fernandez Vargas, E., Garcia Rodriguez, J.J., Greene, H.G., 1977. Active faulting in coastal Almeria (SE Spain) and adjacent continental shelf. In: Seminarios de Tectónica Global. Madrid, Fundación Gómez Pardo, 1-16.

Bell, J.W., Amelung, F., King, G.C.P., 1997. Preliminary late Quaternary slip history of the Carboneras Fault, Southeastern Spain. Journal of Geodynamics, 24(1-4), 51-66.

Boorsma, L.J., 1992. Syn-tectonic sedimentation in a Neogene strike-slip basin containing a stacked Gilbert-type delta (SE Spain). Sedimentary Geology, 81(1-2), 105-123.

Booth-Rea, G., Ranero, C.R., Martínez-Martínez, J.M., Grevemeyer, I., 2007. Crustal types and Tertiary tectonic evolution of the Alborán sea, western Mediterranean. Geochemistry, Geophysics, Geosystems, 8(10), 1-25.

Bousquet, J.C., 1979. Quaternary strike-slip faults in southeastern spain. Tectonophysics, 52(1-4), 277-286.

Bousquet, J.C., Philip, H., 1976. Observations microtectoniques dur la compression nord-sud quaternarie des Cordilleres betiques orientales (Espagne meridionale – Arc de Gibraltar). Bulletin de la Société Géologique de France, S7-XVIII(3), 711-724. DOI: 10.2113/gssgfbull.S7-XVIII.3.711

Bousquet, J.C., Dumas, B., Montenat, C., 1975. Le décrochement de Palomarès: décrochement quaternaire senestre du bassin de Vera (Cordillères bétiques orientales, Espagne). Cuadernos de geología de la Universidad de Granada, 6, 113-119.

Buforn, E., Pro, C., Sanz de Galdeano, C., Cantavella, J.V., Cesca, S., Caldeira, B., Udías, A., Mattesini, M., 2017. The 2016 south Alboran earthquake (Mw=6.4): A reactivation of the Ibero-Maghrebian region? Tectonophysics, 712-713, 704-715.

Calvert, A., Gomez, F., Seber, D., Barazangi, M., Jabour, N., Ibenbrahim, A., Demnati, A., 1997. An integrated geophysical investigation of recent seismicity in the Al-Hoceima region of north Morocco. Bulletin of the Seismological Society of America, 87(3), 637-651.

Comas, M.C., Zahn, R., Klauss, A., (eds.), 1995. Mediterranean Sea II: the western Mediterranean. Ocean Drilling Program, LEG 161 Preliminary report 1-89. [Retrieved: 24/10/2018. Available on: http://www-odp.tamu.edu/publications/prelim/161_Prelim/161PRELIM.PDF]

De Larouzière, F.D., Bolze, J., Bordet, P., Hernandez, J., Montenat, C., Ott d'Estevou, P., 1988. The Betic segment of the lithospheric Trans-Alboran shear zone during the Late Miocene. Tectonophysics, 152(1-2), 41-52.

Echeverria, A., Khazaradze, G., Asensio, E., Masana, E., 2015. Geodetic evidence for continuing tectonic activity of the Carboneras fault (SE Spain). Tectonophysics, 663, 302-309.

Estrada, F., Ercilla, G., Alonso, B., 1997. Pliocene-Quaternary tectonic-sedimentary evolution of the NE Alboran Sea (SW Mediterranean Sea). Tectonophysics, 282(1-4), 423-442.

Faulkner, D.R., Lewis, A.C., Rutter, E.H., 2003. On the internal structure and machanics of large strike-slip fault zones: field observations of the Carboneras fault in southeastern Spain. Tectonophysics, 367(3-4), 235-251.

Fernández-Soler, J.M., 1996. El volcanismo calco-alcalino en el Parque Natural de Cabo de Gata-Níjar (Almería): Estudio volcanológico y petrológico. Monografías medio natural, 2. Almería, Sociedad Almeriense de Historia Natural-Consejería de Medio Ambiente, Junta de Andalucía, 295pp.

Ferrater, M., Ortuño, M., Masana, E., Martínez-Díaz, J.J., Pallàs, R., Perea, H., Baize, S., García-Meléndez, E., Echeverria, A., Rockwell, T., Sharp, W.D., Arrowsmith, R., 2017. Lateral slip rate of Alhama de Murcia fault (SE Iberian Peninsula) based on a morphotectonic analysis: Comparison with paleoseismological data. Quaternary International, 451, 87-100.

Fournier, M., 1980. Le bassin de Nijar-Carboneras (Cordillères bétiques): néotectonique: étude des diaclases. PhD Thesis. Paris, Université Denis Diderot, 157pp.

Frizon de Lamotte, D., Jarrige, J.J., Vidal, J.C., 1980. Le magmatisme Bético-rifain est-il lié à une zone d'accidents décrochants "trans-Alboran". Societe Géologique de France, 8ème Réunion Annuelle des Sciences de la Terre, Marseille, 155.

García-Mayordomo, J., 2005. Caracterización y Análisis de la Peligrosidad Sísmica en el Sureste de España. PhD Thesis. Madrid, Universidad Complutense de Madrid, 373pp.

Goy, J.L., Zazo, C., 1983. Los piedemontes cuaternarios de la región de Almería (España). Análisis morfológico y relación con la neotectónica. Cuadernos del Laboratorio Xeolóxico de Laxe: Revista de xeoloxía galega e do hercínico peninsular, 5, 397-419.

Goy, J.L., Zazo, C., 1986. Synthesis of the quaternary in the almeria littoral neotectonic activity and its morphologic features, weastern betics, Spain. Tectonophysics, 130(1-4), 259-270.

Gràcia, E., Pallàs, R., Soto, J.I., Comas, M., Moreno, X., Masana, E., Santanach, P., Diez, S., García, M., Dañobeitia, J.J., HITS scientific party, 2006. Active faulting offshore SE Spain (Alboran Sea): Implications for Earthquake hazard assessment in the Southern Iberian margin. Earth and Planetary Science Letters, 241(3-4), 734-749.

Gràcia, E., Bartolome, R., Lo Iacono, C., Moreno, X., Stich, D., Martínez-Diaz, J.J., Bozzano, G., Martínez-Loriente, S., Perea, H., Diez, S., Masana, E., Dañobeitia, J.J., Tello, O., Sanz, J.L., Carreño, E., Farran, M., Andara, E., Pérez, S., Román, M.J., 2012. Acoustic and seismic imaging of the Adra Fault (NE Alboran Sea): In search of the source of the 1910 Adra earthquake. Natural Hazards and Earth System Sciences, 12(11), 3255-3267. DOI: 10.5194/nhess-12-3255-2012

Hall, S.H., 1983. Post alpine tectonic evolution of SE Spain and the structure of fault gouges. PhD Thesis. London, Imperial College, University of London, 192pp.

Keller, J.V.A., Hall, S.H., Dart, C.J., McClay, K.R., 1995. The geometry and evolution of a transpressional strike-slip system: the Carboneras fault, SE Spain. Journal of the Geological Society, 152(2), 339-351.

Lafosse, M., d'Acremont, E., Rabaute, A., Mercier de Lépinay, B., Tahayt, A., Ammar, A., Gorini, C., 2017. Evidence of quaternary transtensional tectonics in the Nekor basin (NE Morocco). Basin Research, 29(4), 470-489.

López-Comino, J.-A., Mancilla, F., Morales, J., Stich, D., 2012. Rupture directivity of the 2011, Mw 5.2 Lorca earthquake (Spain). Geophysical Research Letters, 39(3), L03301. DOI: 10.1029/2011GL050498

Maher, E., Harvey, A.M., France, D., 2007. The impact of a major Quaternary river capture on the alluvial sediments of a beheaded river system, the Rio Alias SE Spain. Geomorphology, 84(3-4), 344-356.

Martín, R., Stich, D., Morales, J., de Lis Mancilla, F., 2015. Moment tensor solutions for the Iberian-Maghreb region during the IberArray deployment (2009-2013). Tectonophysics, 663, 261-274.

Martínez-Díaz, J.J., Masana, E., Hernández-Enrile, J.L., Santanach, P., 2003. Effects of repeated paleoeartquakes on the Alhama de Murcia Fault (Betic Cordillera, Spain) on the Quaternary evolution of an alluvial fan system. Annals of Geophysics, 46(5), 775-792.

Martínez-García, P., Comas, M., Soto, J.I., Lonergan, L., Watts, A.B., 2013. Strike-slip tectonics and basin inversion in the Western Mediterranean: the Post-Messinian evolution of the Alboran Sea. Basin Research, 25(4), 361-387.

Martínez-Solares, J.M., Mezcua, J., 2002. Catálogo sísmico de la Península Ibérica (880 a.C.–1900). Madrid, Dirección General del Instituto Geográfico Nacional, Monografia, 253pp.

Masana, E., Martínez-Díaz, J.J., Hernández-Enrile, J.L., Santanach, P., 2004. The Alhama de Murcia fault (SE Spain), a seismogenic fault in a diffuse plate boundary. Seismotectonic implications for the Ibero-Magrebian region. Journal of Geophysical Research, Solid Earth, 109(B1), 1-17.

Mezcua, J., Rueda, J., García Blanco, R.M., 2013. Iberian Peninsula Historical Seismicity Revisited: An Intensity Data Bank. Seismological Research Letters, 84(1), 9-18.

Montenat, C., Ott D'Estevou, P., 1996. Late Neogene basins evolving in the Eastern Betic transcurrent fault zone: an illustrated review. In: Friend, P.F., Dabrio, C.J. (eds.). Tertiary Basins of Spain: The Stratigraphic Record of Crustal Kinematics. Cambridge, Cambridge University Press, 372-386.

Montenat, C., Ott d'Estevou, P.O., Rodríguez Fernández, J.R., Sanz de Galdeano, C., 1990. Geodynamic evolution of the Betic Neogene intramontane basins (S and SE Spain). In: Agustí, J., Domènech, R., Julià, R., Martinell, J. (eds.). Iberian Neogene Basins. Paleontologia i Evolució, Memòria Especial 2, 5-60.

Moreno, X., 2011. Neotectonic and Paleoseismic Onshore-Offshore integrated study of the Carboneras Fault (Eastern Betics, SE Iberia) / Estudio integrado tierra-mar de la Neotectonica y Paleosismología de la Falla de Carboneras (Béticas Orientales, SE Península Ibérica). Ph.D Thesis. Barcelona, Universitat de Barcelona, 365pp.

Moreno, X., Masana, E., Gràcia, E., Pallàs, R., Ruano, P., Coll, M., Štěpančíková, P., Santanach, P., 2007. Primeras evidencias de paleoterremotos en la falla de Carboneras: estudio paleosismológico en el segmento de La Serrata. Geogaceta, 41, 135-138.

Moreno, X., Masana, E., Pallàs, R., Gràcia, E., Rodés, Á., Bordonau, J., 2015. Quaternary tectonic activity of the Carboneras Fault in the La Serrata range (SE Iberia): Geomorphological and chronological constraints. Tectonophysics, 663, 78-94.

Moreno, X., Gràcia, E., Bartolomé, R., Martínez-Loriente, S., Perea, H., de la Peña, L.G., Iacono, C.L., Piñero, E., Pallàs, R., Masana, E., Dañobeitia, J.J., 2016. Seismostratigraphy and tectonic architecture of the Carboneras Fault offshore based on multiscale seismic imaging: Implications for the Neogene evolution of the NE Alboran Sea. Tectonophysics, 689, 115-132.

Niemeijer, A.R., Vissers, R.L.M., 2014. Earthquake rupture propagation inferred from the spatial distribution of fault rock frictional properties. Earth and Planetary Science Letters, 396, 154-164.

Ortuño, M., Masana, E., Garcia-Melendez, E., Martínez-Díaz, J.J., Štěpančíková, P., Cunha, P.P., Sohbati, R., Canora, C., Buylaert, J.-P., Murray, A.S., 2012. An exceptionally long paleoseismic record of a slow-moving fault: The Alhama de Murcia fault (Eastern Betic shear zone, Spain). Geological Society of America Bulletin, 124(9-10), 1474-1494.

Pedrera, A., de Lis Mancilla, F., Ruiz-Constán, A., Galindo-Zaldívar, J., Morales, J., Arzate, J., Marín-Lechado, C., Ruano, P., Buontempo, L., Anahnah, F., Stich, D., 2010. Crustal-scale transcurrent fault development in a weak-layered crust from an integrated geophysical research: Carboneras Fault Zone, eastern Betic Cordillera, Spain. Geochemistry, Geophysics, Geosystems, 11(12), 1-24. DOI: 10.1029/2010gc003274

Perea, H., Gràcia, E., Alfaro, P., Bartolomé, R., Lo Iacono, C., Moreno, X., Masana, E., EVENT-SHELF Team, 2012. Quaternary active tectonic structures in the offshore Bajo Segura basin (SE Iberian Peninsula - Mediterranean Sea). Natural Hazards and Earth System Sciences, 12(10), 3151-3168.

Pineda, A., Giner, J., Goy, J.L., Zazo, C., 1981. Mapa geológico de España. 1:50,000. 2a Serie MAGNA, 1046 (Carboneras). Madrid, Instituto Geológico y Minero de España.

Reicherter, K., Hübscher, C., 2007. Evidence for a seafloor rupture of the Carboneras Fault Zone (southern Spain): Relation to the 1522 Almería earthquake? Journal of Seismology, 11(1), 15-26.

Reilinger, R., McClusky, S., 2011. Nubia–Arabia–Eurasia plate motions and the dynamics of Mediterranean and Middle East tectonics. Geophysical Journal International, 186(3), 971-979.

Rodés, Á., Pallàs, R., Braucher, R., Moreno, X., Masana, E., Bourlés, D.L., 2011. Effect of density uncertainties in cosmogenic [10]Be depth-profiles: Dating a cemented Pleistocene alluvial fan (Carboneras Fault, SE Iberia). Quaternary Geochronology, 6(2), 186-194.

Rodríguez-Escudero, E., 2017. Implicaciones de la Estructura Interna de una Zona de Falla Activa en la Génesis de Terremotos. PhD Thesis. Madrid, Universidad Autónoma de Madrid, 294pp.

Rodríguez-Escudero, E., Martínez-Díaz, J.J., Álvarez-Gómez, J.A., Insua-Arévalo, J.M., Capote, R., 2014. Tectonic setting of the recent damaging seismic series in the Southeastern Betic Cordillera, Spain. Bulletin of Earthquake Engineering, 12(5), 1831-1854.

Rutter, E.H., Maddock, R.H., Hall, S.H., White, S.H., 1986. Comparative microstructures of natural and experimentally produced clay-bearing fault gouges. Pure and applied geophysics, 124(1-2), 3-30. DOI: 10.1007/BF00875717

Rutter, E.H., Faulkner, D.R., Burgess, R., 2012. Structure and geological history of the Carboneras Fault Zone, SE Spain: Part of a stretching transform fault system. Journal of Structural Geology, 45, 68-86.

Sanz de Galdeano, C., 1990. Geologic evolution of the Betic Cordilleras in the Western Mediterranean, Miocene to the present. Tectonophysics, 172(1-2), 107-119.

Santisteban, J.I., Schulte, L., 2007. Fluvial networks of the Iberian Peninsula: a chronological framework. Quaternary Science Reviews, 26(22-24), 2738-2757.

Schulte, L., 2002. Evolución cuaternaria de la depresión de Vera y de Sorbas oriental (SE-Península Ibérica): reconstrucción de las fluctuaciones paleoclimáticas a partir de estudios morfológicos y edafológicos. PhD Thesis. Barcelona, Universitat Barcelona, 251pp.

Scotney, P., Burguess, R., Rutter, E.H., 2000. ^{40}Ar/^{39}Ar age of the Cabo de Gata volcanic series and displacements on the Carboneras fault zone, SE Spain. Journal of the Geological Society, 157(5), 1003-1008.

Silva, P.G., Goy, J.L., Zazo, C., Bardají, T., 2003. Fault-generated mountain fronts in southeast Spain: geomorphologic assessment of tectonic and seismic activity. Geomorphology, 50(1-3), 203-225.

Stich, D., Ammon, C.J., Morales, J., 2003a. Moment tensor solutions for small and moderate earthquakes in the Ibero-Maghreb region. Journal of Geophysical Research: Solid Earth, 108(B3), 2148. DOI: 10.1029/2002JB002057

Stich, D., Batlló, J., Morales, J., Macià, R., Dineva, S., 2003b. Source parameters of the MW=6.1 1910 Adra earthquake (southern Spain). Geophysical Journal International, 155(2), 539-546.

Tahayt, A., Feigl, K.L., Mourabit, T., Rigo, A., Reilinger, R., McClusky, S., Fadil, A., Berthier, E., Dorbath, L., Serroukh, M., Gomez, F., Ben Sari, D., 2009. The Al Hoceima (Morocco) earthquake of 24 February 2004, analysis and interpretation of data from ENVISAT ASAR and SPOT5 validated by ground-based observations. Remote Sensing of Environment, 113(2), 306-316.

Udías, A., López-Arroyo, A., Mezcua, J., 1976. Seismotectonic of the Azores-Alboran region. Tectonophysics, 31(34), 259-289.

Vegas, R., 1992. Sobre el tipo de deformación distribuida en el contacto Africa y la Península Ibérica. Física la Tierra, 4, 41-56.

Vera, J.A., 2000. El Terciario de la Cordillera Bética: estado actual de conocimientos. Revista de la Sociedad Geológica de España, 13(2), 345-373.

Vissers, R.L.M., Meijninger, B.M.L., 2011. The 11 May 2011 earthquake at Lorca (SE Spain) viewed in a structural-tectonic context. Solid Earth, 2, 199-204. DOI: 10.5194/se-2-199-2011

Weijermars, R., 1987. The construction of shear strain profiles across brittle-ductile shears. Preliminary estimates of conventional shear strain rates for the Truchas and Palomares shears (Spain) and the Alpine Fault (New Zeland). Annales Geophysicae, B, 5(2), 201-210.

Weijermars, R., 1991. Geology and tectonics of the Betic Zone, SE Spain. Earth-Science Reviews, 31(3-4), 153-236.

Wells, K., Coppersmith, D.L., 1994. New empirical relationships among magnitude, rupture length, rupture width, rupture area, and surface displacement. Bulletin of the Seismological Society of America, 84, 974-1002.